Cooperative Sensing Assisted Joint Transmission for Ground-to-Air Communication Systems

Jiahui Zhang*, Zesong Fei*, Xinyi Wang*, Peng Liu*, Jingxuan Huang*, Guohua Wei*, Weijie Yuan†
*School of Information and Electronics, Beijing Institute of Technology (BIT), Beijing 100081, China
† Department of Electrical and Electronics Engineering, Southern University of Science and Technology, Shenzhen 518055, China
Emails: zjh20210920@163.com, feizesong@bit.edu.cn, bit_wangxy@163.com, bit_peng_liu@163.com,
jxhbit@gmail.com, ghwei@bit.edu.cn, yuanwj@sustech.edu.cn.

***Abstract*—Cooperative sensing and cooperative communications are viewed as promising techniques for improving the sensing and communication performance by utilizing the space diversity. In this paper, we investigate the cooperative-sensing assisted joint transmission for a ground-to-air system. By cooperatively processing the echoes from different UAVs, we propose a cooperative sensing scheme based on the extended Kalman filtering mechanism. To improve the system sum-rate based on the cooperative tracking information, we jointly optimize the transmit beam power of different BSs via a teaching-and-learning based optimization technique. Numerical results show that compared with the conventional separate sensing scheme, the proposed cooperative sensing scheme is able to significantly improve the positioning accuracy, thereby improving the communication performance.**

***Index Terms*—Unmanned aerial vehicles, cooperative sensing, sensing-assisted communication, joint transmission.**

I. Introduction

Unmanned aerial vehicles (UAVs), as a promising technique, viewed as key enablers for executing various tasks in future [1], such as data sensing, military reconnaissance, and formation flight. In order to guarantee the safety of UAVs and satisfy various mission-specific requirements, it is necessary to ensure the high-capacity and low-latency data transmission between UAVs and base stations (BSs) [2].

The joint transmission (JT) technique, in which multiple BSs transmit signals to one or multiple user(s), can significantly enhance the robustness and throughput of the communication links, especially for users at the cell edge, which have been studied in [2]–[4]. To support joint transmission, accurate channel estimation is of great importance. However, due to the high mobility of UAVs, conventional pilot based channel estimation schemes faces the problem of "channel aging", therefore cannot provide accurate channel state information (CSI). Fortunately, the rising of the integrated communication and sensing (ISAC) technique allow simultaneously performing sensing and communication functionalities based on one unified waveform, which facilitates the sensing-aided communication [5]–[8]. Compared with the pilot based CSI acquisition mechanism, the sensing-aided mechanism is able to significantly improve the throughput by saving the pilot overhead. Moreover, it allows continuous CSI acquisition.

However, it should be noted that the accuracy of CSI reconstruction is closely related to the sensing accuracy, while the sensing accuracy and robustness of a single BS are limited. Facing this issue, by employing multiple BSs as distributed sensing nodes, which share sensing information to enable collaborative processing, the cooperative sensing (co-sensing) technique is able to improve the sensing accuracy. The authors in [9] proposed OFDM-based co-sensing with multiple single-antenna BSs, and provided a maximum-likelihood based algorithm to achieve multi-target association. The authors in [10] demonstrated the sensing information fusion of two multi-antenna nodes and verified the improvement of co-sensing on sensing performance. Furthermore, the authors in [11] studied the employment of extended Kalman filter (EKF) in co-sensing.

Although the above works have studied joint transmission and cooperative sensing, respectively, their integration and the impacts of co-sensing on JT have not been studied. In this paper, we study the cooperative sensing assisted joint transmission, in which multiple BSs coherently transmit signals to multiple UAVs based on the sensing results. By employing the ISAC waveform, the BSs are able to estimate the time-variant locations of UAVs based on the echos, thereby reconstructing their CSI. To achieve CSI prediction, the EKF technique is applied to cooperatively process the sensing information of multiple BSs. Subsequently, in each time slot, the power of the transmit beams are jointly optimized for maximizing the system sum-rate, under the sensing signal-to-clutter-noise-ratio (SCNR) and transmit power constraints. We first transform this non-convex problem into appropriate forms, then apply a teaching-and-learning optimization algorithm to address it. Numerical results show cooperative sensing can achieve more accurate positioning than separate sensing; thereby, the system sum rate achieved by co-sensing assisted JT (CSJT) outperforms that of the separate sensing assisted JT (SSJT).

II. System Model

In this section, we first describe the considered system model. Then we present the signal model of coherent transmission. Afterwards, the signal model of the received echos is provided.

A. System Description

We consider the co-sensing assisted JT system, as shown in Fig. 1, which consists of M BSs denoted by $\mathcal{M} = \{1, ..., M\}$, K UAVs, denoted by $\mathcal{K} = \{1, ..., K\}$. UAVs maneuver over the BSs, and the BSs coherently transmit orthogonal frequency division multiplexing (OFDM) signal to the UAVs. The locations of BSs are denoted as $\mathbf{q}_m = [x_m, y_m, 0]$, while the trajectories of UAVs are denoted as $\mathbf{x}_k[n] =$

This work was supported by the National Key R&D Program of China under Grant No. 2021YFB2900200, and the National Natural Science Foundation of China under Grant U20B2039. Corresponding author: ZeSong Fei.

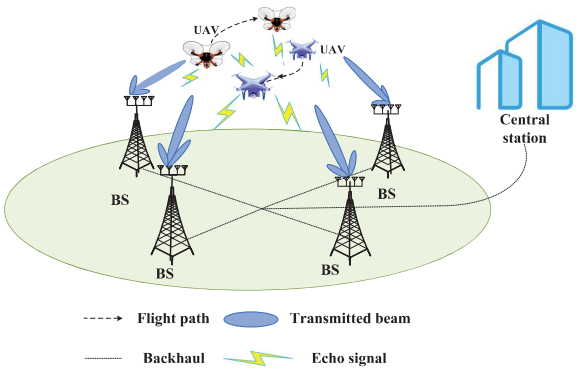

Fig. 1. An illustration of the considered co-sensing assisted JT in ISAC system.

$[x_k[n], y_k[n], z_k[n]]$, $k = \{1, ..., K\}$, with the corresponding speeds expressed as $\mathbf{v}_k[n] = [v_k[n], v_k[n], v_k[n]]$. Each BS is equipped with two uniform planar arrays (UPAs) for signal transmission and reception, with the antenna number being N_t and N_R, respectively. Without loss of generality, we assume $N_t = N_r = N_x \times N_y$. The steering vector of UPAs is expressed as

$$\mathbf{a}(\theta, \phi) = \text{vec}\left(\mathbf{A}\left(\theta, \phi\right)\right), \tag{1}$$

which vec$(\cdot)$ represents the operation of converting matrix into column vector, and $\mathbf{A}\left(\theta, \phi\right) \in \mathbb{C}^{N_y \times N_x}$ with each element as

$$\mathbf{A}\left(a_x, a_y\right) = e^{j((a_y-1)\beta + (a_x-1)\alpha)} \tag{2}$$

in which $\alpha = \frac{2\pi}{\lambda} d_1 \sin(\phi)\sin(\theta)$, $\beta = \frac{2\pi}{\lambda} d_2 \cos(\phi)$ with d_1 and d_2 denoting the horizontal and vertical intervals between adjacent antennas, and λ is the wavelength of the carrier signal.

To enable cooperative sensing and coherent transmission, all BSs are connected to a central station via backhaul [9]. Through transmitting the ISAC signals, the BSs receive the echoes from UAVs, and upload the sensing information to the central station for cooperative sensing. The bandwith allocated to each BS is denoted by B. The power of the beams transmitted by BSs are denoted as $\mathbf{p} = [p_{1,1}, \cdots, p_{1,K}; \cdots; p_{M,1}, \cdots, p_{M,K}]^T$, where $p_{m,k}$ represents the transmission power from BS m to UAV k. To address the high mobility of UAVs, the BSs also conduct beam prediction based on the sensing information, thereby facilitating the co-sensing assisted joint transmission. We consider a duration T of interest, which is discretized into N time slots with $\Delta T = T/N$.

B. Joint Transmission Model

In the n-th slot, M BSs jointly transmit data streams $\mathbf{s}[n] = [s_1[n], ..., s_K[n]]^T$ to K UAVs. To reduce inter-cell interference in JT, each stream transmitted by BSs adopts space-frequency/time block coding (SFBC/STBC) [12], [13]. The OFDM stream of the m-th BS is expressed as

$$\mathbf{s}_m[n] = [s_{m,1}[n], ..., s_{m,K}[n]]^T \tag{3}$$

The transmitted signal from the m-th BS is expressed as

$$\tilde{\mathbf{s}}_m[n] = \mathbf{F}_m[n]\mathbf{s}_m[n] \in \mathbb{C}^{N_t \times 1}, \tag{4}$$

where $\mathbf{F}_m[n] = [\mathbf{f}_{m,1}[n], ..., \mathbf{f}_{m,K}[n]] \in \mathbb{C}^{N_t \times K}$ denotes m-th BS's transmit beamforming matrix in the n-th slot, which is designed based on sensing and prediction information. Specifically, $\mathbf{f}_{m,k}[n]$ is given by

$$\mathbf{f}_{m,k}[n] = \mathbf{a}(\hat{\theta}_{m,k}[n|n-1], \hat{\phi}_{m,k}[n|n-1]), \tag{5}$$

where $\hat{\theta}_{m,k}[n|n-1]$ and $\hat{\phi}_{m,k}[n|n-1]$ respectively denote the predicted horizontal and vertical angles of the k-th UAV in the n-th slot.

The path loss from BS m to UAV k follows the free-space path loss model, which is given by

$$h_{m,k}[n] = \sqrt{\rho_0 \left\|\mathbf{d}_{m,k}[n]\right\|^{-2}}, \tag{6}$$

where $\mathbf{d}_{m,k}[n] = \mathbf{x}_k[n] - \mathbf{q}_m$, $\|\cdot\|$ denotes its norm, and ρ_0 denotes the path loss at the reference distance d_0 = 1 m.

For convenience, the subscript n is omitted below. The signal received by the k-th UAV can be expressed as equation (7), where $\tau_{m,k}$, $u_{m,k}$, $\theta_{m,k}$, and $\varphi_{m,k}$ respectively denote the time delay, Doppler shift, horizontal angle and vertical angle between BS m and UAV k, $\mathcal{W}_k$ denotes the set of BSs serving UAV k, $\mathcal{T}_m$ denotes the set of UAVs served by BS m_2, and $n_k \sim \mathcal{CN}\left(0, \sigma_k^2\right)$ denotes the additive white Gaussian noise (AWGN) at UAV k. $\tau_{m,k}$, $u_{m,k}$, $\theta_{m,k}$, and $\varphi_{m,k}$ are respectively given as

$$\begin{aligned} \tau_{m,k} &= \frac{\|\mathbf{d}_{m,k}\|}{c}, \qquad \theta_{m,k} = \arcsin\left(\frac{y_k - y_m}{\|\mathbf{r}_{m,k}\|}\right), \\ u_{m,k} &= \frac{\mathbf{v}_k^T \mathbf{d}_{m,k} f_c}{c\|\mathbf{d}_{m,k}\|}, \quad \phi_{m,k} = \arcsin\left(\frac{z_k}{\|\mathbf{d}_{m,k}\|}\right), \end{aligned} \tag{8}$$

in which $\mathbf{v}_k^T \mathbf{d}_{m,k}/\|\mathbf{d}_{m,k}\|$ denotes the radial speed of the UAV k relative to BS m, $\mathbf{r}_{m,k} = \|[x_k, y_k] - [x_m, y_m]\|$. f_c and c respectively denote carrier frequency and light speed.

After SFBC decoding, the signal-to-interference-plus-noise ratio (SINR) of the received downlink (DL) communication signal at UAV k is expressed as [14]

$$\gamma_{u_k} = \frac{\xi \sum\limits_{m_1 \in \mathcal{W}_k} \left|\sqrt{p_{m_1,k}} h_{m_1,k} \mathbf{a}_{m_1,k}^H \mathbf{f}_{m_1,k}\right|^2}{\sum\limits_{k_2 \in \mathcal{T}_{m_2}, k_2 \neq k} \sum\limits_{m_2 \in \mathcal{W}_k} \left|\sqrt{p_{m_2,k_2}} h_{m_2,k} \mathbf{a}_{m_2,k}^H \mathbf{f}_{m_2,k_2}\right|^2 + \sigma_k^2}. \tag{9}$$

where ξ denotes the encoding rate, $\mathbf{a}_{m,k}^H$ denotes $\mathbf{a}^H(\theta_{m,k}, \phi_{m,k})$.

The communication data rate for UAV k is expressed as

$$R_k = \log_2(1 + \gamma_{u_k}). \tag{10}$$

C. Co-sensing Signal Model

In the n-th slot, echo signal received by the BS m is expressed as (11), where $n_m \sim \mathcal{CN}\left(0, \sigma_m^2\right)$ represents the AWGN at BS m, $h_{m_2,k,m}$ and $h_{m_2,k,m}$ denote the path loss of 'BS m-UAV k-BS m' and 'BS m_2-UAV k-BS m', which are respectively given separately as

$$h_{m,k,m} = \psi_0 \sqrt{\rho_0 (4\pi)^{-2} \|\mathbf{d}_{m,k}\|^{-4}}, \tag{12}$$

$$h_{m_2,k,m} = \psi_0 \sqrt{\rho_0 \|\mathbf{d}_{m_2,k}\|^{-2} (4\pi \|\mathbf{d}_{m,k}\|)^{-2}}, \tag{13}$$

in which ψ_0 denotes the radar cross section (RCS).

After sensing SFBC decoding [15], the monostatic echoes can be retained while the bistatic echoes can be eliminated

$$y_{c_k} = \sum_{m_1 \in \mathcal{W}_k} \left\{ \sqrt{p_{m_1,k}} h_{m_1,k} \mathbf{a}^H(\theta_{m_1,k}, \phi_{m_1,k}) \mathbf{f}_{m_1,k} \; s_{m_1,k}\left(t - \tau_{m_1,k}\right) e^{j2\pi\mu_{m_1,k}t} \right\} + \sum_{k_2 \in \mathcal{T}_{m_2}, k_2 \neq k} \sum_{m_2 \in \mathcal{W}_k} \left\{ \sqrt{p_{m_2,k_2}} h_{m_2,k} \mathbf{a}^H(\theta_{m_2,k}, \phi_{m_2,k}) \mathbf{f}_{m_2,k_2} \; s_{m_2,k_2}\left(t - \tau_{m_2,k}\right) e^{j2\pi\mu_{m_2,k}t} \right\} + n_k \tag{7}$$

$$y_{s_m} = \sum_{k_1 \in \mathcal{T}_m} \left\{ \sqrt{p_{m,k_1}} h_{m,k_1,m} \mathbf{b}(\theta_{m,k_1}) \; \mathbf{a}^H_{m,k_1} \mathbf{f}_{m,k_1} s_{m,k_1}(t - 2\tau_{m,k_1}) e^{j2\pi\mu_{m,k_1}t} \right\} + \sum_{m_2 \in \mathcal{W}_{k_2}, m_2 \neq m} \sum_{k_2 \in \mathcal{T}_m} \left\{ \sqrt{p_{m_2,k_2}} h_{m_2,k_1,m} \mathbf{b}(\theta_{m,k_2}) \; \mathbf{a}^H_{m_2,k_2} \mathbf{f}_{m_2,k_2} s_{m_2,k_2}(t - \tau_{m_2,k_2} - \tau_{m,k_2}) e^{j2\pi\mu_{m,k_2}t} \right\} + n_m \tag{11}$$

in the corresponding frequency band. Therefore, the signal-to-clutter-plus-noise ratio (SCNR) of the received echo signal of BS m for UAV k is xpressed as

$$\gamma_{s_{m,k}} = \frac{G_r \left| \sqrt{p_{m,k}} h_{m,k,m} \mathbf{a}^H_{m,k} \mathbf{f}_{m,k} \right|^2}{\sum_{k_2 \in \mathcal{T}_m, k_2 \neq k} \left| \sqrt{p_{m,k_2}} h_{m,k_2,m} \mathbf{a}^H_{m,k_2} \mathbf{f}_{m,k_2} \right|^2 + \sigma_m^2}, \tag{14}$$

where G_r devotes the angle matching gain.

III. Cooperative Sensing Based on EKF

In this section, we propose an Extended Kalman Filter (EKF) based cooperative sensing technique. We first present the measurement model of the BSs based on the received signal model. Subsequently, the beam and target association issues are discussed. Afterwards, the detailed procedure of EKF based cooperative sensing is presented.

A. Measurement Model

Based on the downlink signal echo, BSs can obtain the observable parameters of UAVs. We use $\bar{\tau}_{m,k}$,$\bar{u}_{m,k}$,$\bar{\theta}_{m,k}$, and $\bar{\varphi}_{m,k}$ to represent the time delay, Doppler shift, horizontal angle and vertical angle observed by the BS m on UAV k respectively. The measurement models of observable parameters are shown as follows.

$$\begin{aligned} \bar{\tau}_{m,k} &= 2\tau_{m,k} + z_{\tau_{m,k}}, \quad & \sin\bar{\theta}_{m,k} &= \sin\theta_{m,k} + z_{\sin\theta_{m,k}}, \\ \bar{u}_{m,k} &= 2u_{m,k} + z_{f_{m,k}}, \quad & \sin\bar{\phi}_{m,k} &= \sin\phi_{m,k} + z_{\sin\phi_{m,k}}, \end{aligned} \tag{15}$$

where $\tau_{m,k}$, $u_{m,k}$, $\theta_{m,k}$, and $\varphi_{m,k}$ are given in (8), and $z_{\tau_{m,k}}$, $z_{u_{m,k}}$, $z_{sin\theta_{m,k}}$, and $z_{sin\varphi_{m,k}}$ represent the measurement error, which subject to uniform distribution with zero mean and the following standard deviation.

$$\begin{aligned} \sigma_{\tau_{m,k}} &= \frac{1}{B \times \sqrt{2\gamma_{s_{m,k}}}}, & \sigma_{\theta_{m,k}} &= \frac{\theta_{3dB}\cos\theta_{m,k}}{1.6\sqrt{2\gamma_{s_{m,k}}}}, \\ \sigma_{u_{m,k}} &= \frac{\lambda}{\Delta T \times \sqrt{2\gamma_{s_{m,k}}}}, & \sigma_{\phi_{m,k}} &= \frac{\phi_{3dB}\cos\phi_{m,k}}{1.6\sqrt{2\gamma_{s_{m,k}}}}, \end{aligned} \tag{16}$$

where θ_{3dB} and ϕ_{3dB} respectively devote the horizontal and vertical beam width.

We recast the measure model in (15) as

$$\boldsymbol{\varepsilon}_{m,k} = \mathbf{h}_m(\mathbf{g}_k) + \mathbf{z}_{m,k}, \tag{17}$$

where $\mathbf{g}_k = \left[(\mathbf{x}_k)^T, (\mathbf{v}_k)^T \right]^T$, and

$$\boldsymbol{\varepsilon}_{m,k} = \left[\bar{\tau}_{m,k}, \bar{f}_{m,k}, sin\bar{\theta}_{m,k}, sin\bar{\phi}_{m,k} \right]^T,$$

$$\mathbf{z}_{m,k} = \left[z_{\tau_{m,k}}, z_{u_{m,k}}, z_{sin\theta_{m,k}}, z_{sin\phi_{m,k}} \right]^T.$$

The covariance matrix of $\mathbf{z}_{m,k}$ can be expressed as

$$\mathbf{Q}_{z_{m,k}} = \text{diag}\left[\sigma^2_{\tau_{m,k}}, \sigma^2_{u_{m,k}}, \sigma^2_{sin\theta_{m,k}}, \sigma^2_{sin\phi_{m,k}} \right]. \tag{18}$$

To linearize $\mathbf{h}_m(\mathbf{g}_k)$, we calculate its Jacobian matrix, which can be expressed as

$$\boldsymbol{\eta}_{m,k} = \frac{\partial \mathbf{h}_m}{\partial \mathbf{g}_k} \in \mathbb{C}^{4\times 6}, \tag{19}$$

Specific expressions are as [8].

For UAV k, we set

$$\mathbf{H}(\cdot) = \left[\mathbf{h}_1(\cdot)^T, \mathbf{h}_2(\cdot)^T, ..., \mathbf{h}_M(\cdot)^T \right]^T \in \mathbb{C}^{4M\times 1}, \tag{20}$$

$$\boldsymbol{\Pi}_k = \left[\boldsymbol{\varepsilon}^T_{1,k}, \boldsymbol{\varepsilon}^T_{2,k}, ..., \boldsymbol{\varepsilon}^T_{M,k} \right]^T \in \mathbb{C}^{4M\times 1}, \tag{21}$$

$$\mathbf{Z}_k = \left[\mathbf{z}^T_{1,k}, \mathbf{z}^T_{2,k}, ..., \mathbf{z}^T_{M,k} \right]^T \in \mathbb{C}^{4M\times 1}, \tag{22}$$

$$\mathbf{Q}_{z_k} = \text{diag}\left\{ \mathbf{Q}_{z_{1,k}}, \mathbf{Q}_{z_{2,k}}, \cdots \mathbf{Q}_{z_{M,k}} \right\} \in \mathbb{C}^{4M\times 4M}, \tag{23}$$

$$\boldsymbol{\eta}_k = \frac{\partial \mathbf{H}}{\partial \boldsymbol{\Pi}_k} = \text{diag}\left\{ \eta_{1,k}, \eta_{2,k}, \cdots, \eta_{M,k} \right\} \in \mathbb{C}^{4M\times 4M}. \tag{24}$$

Thus, we have

$$\boldsymbol{\Pi}_k = \mathbf{H}_k(\mathbf{g}_k) + \mathbf{Z}_k. \tag{25}$$

B. Beam and Target Association

While tracking multiple targets with a single BS, a critical issue is the beam association in different time slots, which can be realized by minimizing Euclidean distance between the measurement state and prediction state [5]. For cooperative sensing with multiple BSs, besides beam association, there is also a target association problem. Specifically, the observations from different BSs may not correspond to the same target in the same time slot. By defining the coordinates of UAVs estimated by BSs as $\bar{\mathbf{x}}_{i,1}$, the target association problem can be formulated as [9]

$$j = \arg\min_j \left\| \bar{\mathbf{x}}_{j,m} - \bar{\mathbf{x}}_{i,1} \right\|, i = \{1, \cdots, K\}, \tag{26}$$

where $\bar{\mathbf{x}}_{j,m}$ denotes the j-th coordinates estimated by BS m. Both beam association and target association can be solved via the data correlation technique, which has been studied in [16].

C. Cooperative Tracking Based on EKF

While utilizing the EKF method to jointly estimate and predict the target position, the state evolution model is given by

$$\begin{aligned}\mathbf{g}_k[n+1|n] &= \mathbf{\Delta}[n+1|n]\mathbf{g}_k[n] + \mathbf{w}_k[n+1] \\ \mathbf{\Delta}[n+1|n] &= \begin{bmatrix}\mathbf{I}_3, \mathbf{I}_3\Delta T \\ \mathbf{0}_3,\ \mathbf{I}_3\end{bmatrix}\end{aligned} \tag{27}$$

where $\mathbf{\Delta}[n+1|n]$ denotes the state transition matrix for predicting the target's state in slot $(n+1)$ based on the state in slot n, $\mathbf{I}_3$ and $\mathbf{0}_3$ are 3×3 identity matrix and zero matrix, and $\mathbf{w}_k[n] = \left[w_x, w_y, w_z, w_{v_x}, w_{v_y}, w_{v_z}\right]^T$ denotes the noise term, where the elements are assumed to be independent Gaussian noise with variances of $\sigma_x^2, \sigma_y^2, \sigma_z^2, \sigma_{v_x}^2, \sigma_{v_y}^2, \sigma_{v_z}^2$, respectively. The covariance matrix of $\mathbf{w}_k[n+1]$ is given by

$$\mathbf{Q}_w = diag\left[\sigma_x^2, \sigma_y^2, \sigma_z^2, \sigma_{v_x}^2, \sigma_{v_y}^2, \sigma_{v_z}^2\right] \tag{28}$$

The predicted mean square error (MSE) matrix can be given by

$$\mathbf{M}_k[n+1|n] = \mathbf{\Delta}[n+1|n]\mathbf{M}_k[n]\mathbf{\Delta}^H[n+1|n] \tag{29}$$

The Kalman gain matrix is then calculated as

$$\begin{aligned}&\mathbf{K}_k[n+1] = \mathbf{M}_k[n+1|n]\boldsymbol{\eta}_k^H[n+1]\times \\ &\left(\mathbf{Q}_{z_k} + \boldsymbol{\eta}_k[n+1]\mathbf{M}_k[n+1|n]\boldsymbol{\eta}_k^H[n+1]\right)^{-1}\end{aligned} \tag{30}$$

where $\boldsymbol{\eta}_k[n+1] = \boldsymbol{\eta}_k|_{\boldsymbol{g}[n+1|n]}$.

Finally, based on (25), we can obtain the UAVs' states based on observation parameters in $(n+1)$-th slot slot, with the states and MSE matrix updated as

$$\mathbf{g}_k[n+1] = \mathbf{g}_k[n+1|n] + \mathbf{K}_k[n+1](\mathbf{\Pi}_k[n+1] - \mathbf{H}(\mathbf{g}_k[n+1|n])) \tag{31}$$

$$\mathbf{M}_k[n+1] = (\mathbf{I} - \mathbf{K}_k[n+1]\boldsymbol{\eta}_k[n+1])\mathbf{M}[n+1|n] \tag{32}$$

IV. Transmit Beam Power Optimization

According to (9) and (14), the transmit beams' powerhas great impact on both communication and sensing performance. Therefore, in this section, we investigate the power optimization for the transmit beams

A. Problem Formulation

We focus on jointly optimizing the power for transmit beams in the $(n+1)$-th slot based on the prediction information in the n-th slot, with the aim of maximizing the total predicted communication sum-rate in the $(n+1)$-th slot, while ensuring that the sensing SCNR is greater than a predefined threshold and meets the power constraints. The optimization problem in the n-th slot is formulated as

$$\max_{\mathbf{p}[n+1]} \sum_{k=1}^{K} \log_2\left(1+\gamma_k[n+1|n]\right) \tag{33}$$

$$s.t. \gamma_{s_{m,k}}[n+1|n] \geq \Gamma, \forall m \in \mathcal{M} \tag{33a}$$

$$p_{\min} \leq p_{m,k}[n+1] \leq p_{\max},\ \forall k \in \mathcal{K} \tag{33b}$$

where Γ denotes the sensing SCNR threshold, $p_{\min}$ and $p_{\max}$ are the minimum and maximum values of transmitted beam power respectively.

B. Teaching-Learning-Based Optimization

Note that the above problem is challenging to solve, due to the high non-convexity of objective function (33) and constraint (33a). To address this issue, we utilize a meta-heuristic algorithm called teaching-learning-based optimization (TLBO) method [17]. Firstly, the TLBO model generate U learners. Each learner represents one power optimization scheme [18], which is called knowledge and expressed $\mathbf{p}_u \in \mathbb{C}^{1\times KM}$.

Then we define the fitness function for problem (33) as

$$F\left(\mathbf{p}_u\right) = \sum_{k=1}^{T} \log_2\left(1+\gamma_k[n+1|n]\big|_{\mathbf{p}_u}\right) - \sum_{i=1}^{3} \varsigma_i f_i, \tag{34}$$

with the following penalty functions.

$$\begin{aligned}f_1 &= \sum_{m=1}^{M}\sum_{k=1}^{K}\left(\left[\gamma_{s_{m,k}}[n+1|n] - \Gamma\right]^-\right)^2, \\ f_2 &= \sum_{m=1}^{M}\sum_{k=1}^{K}\left(\left[p_{m,k|u} - p_{\min}\right]^-\right)^2, \\ f_3 &= \sum_{m=1}^{M}\sum_{k=1}^{K}\left(\left[p_{\max} - p_{m,k|u}\right]^-\right)^2.\end{aligned} \tag{35}$$

where ς_i denotes the penalty factor and $[a]^- \triangleq \min\{0, a\}$.

The TLBO method mainly include teaching and learning stages. In the teaching stage, the best learner $u^* = \max_u \{F(\mathbf{p}_u)\}$ is identifid as a teacher to help learners get new knowledge. The output of the teaching stage is also the input of the learning stage. In the learning stage, learners interact to update knowledge. The output of the learning stage will be the input of the teaching phase in the next iteration. The teaching and learning stages are optimized iteratively until $F\left(\mathbf{p}_{u^*}^i\right)$ converges. For further details, we refer the readers to [17].

V. Simulation Results

In this section, we evaluate the performance of the proposed co-sensing assisted JT (CSJT) in ISAC system via numerical simulation. In particular, we take $M=4$, $K=2$ as an example. The coordinates of the BSs are respectively set as $[0,0,0]^T$m, $[0,100,0]^T$m, $[100,0,0]^T$m and $[100,100,0]^T$m. The two UAVs maneuver over $[50\pm 20, 50\pm 20]^T$m at the speed of 20 m/s at the altitudes of 40m and 50m respectively. And the spectrum density of σ_k^2 and σ_m^2 are set to -30dBm/MHz. The maximum and minimum transmit power of BSs are respectively set as 0.5W and 10W. Besides, we set $f_c = 1.8$GHz, $\rho_0 = -60$dB, $\xi = 3/4$, $T = 3$s, $N_x = 2$, $\theta_{3dB} = \phi_{3dB} = 0.3$rad, $\Gamma = -10 \sim 7$dB, $\psi_0 = 20$dBsm, $G_r = 10$dB. For comparison, we also consider the case that each BS utilizes its independent sensing information to assist joint, recorded as "Separate sensing assisted JT (SSJT)".

In Fig. 2(a), we show the average positioning error versus bandwidth with $N_y = 64$. Compared with separate sensing, the average positioning error of co-sensing is significantly decreased. Meanwhile, the positioning error of the co-sensing scheme decreases with the bandwidth increase, while positioning error decreases slightly within the limited bandwidth variation range for the separate sensing scheme. At the same

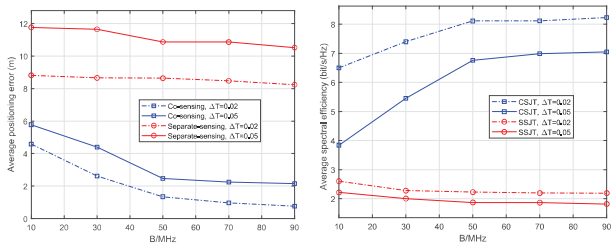

(a) (b)

Fig. 2. (a) Average positioning error versus bandwidth ($N_y = 64$). (b) Average spectral efficiency versus bandwith ($N_y = 64$).

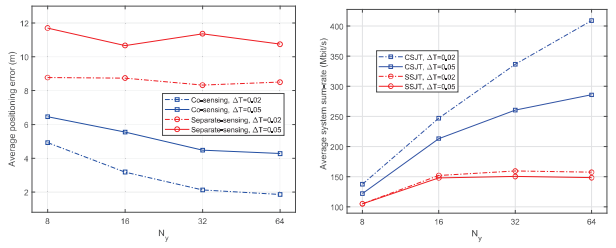

(a) (b)

Fig. 3. (a) Average positioning error versus horizontal antenna dimension ($B = 50$MHz). (b) Average system sum-rate versus horizontal antenna dimension ($B = 50$MHz).

time, we observe that smaller slot ΔT results in better positioning results for both co-sensing and separate sensing.

To show the gain of co-sensing in improving communication performance, we show the average spectral efficiency in Fig. 2(b). With the bandwidth increasing, the average spectral efficiency of the proposed CSJT scheme increases fast, especially for a small bandwidth since the corresponding positioning error is significantly decreased. Although the positioning error also decreases at 50-90MHz, its impact on beam alignment is smaller. However, for SSJT, the average spectral efficiency is slightly reduced with the bandwidth increasing. This is because the decrease of positioning error is limited, while greater noise power is introduced due to the increased bandwidth. Again, smaller slot ΔT result in higher average system sum-rate for both schemes due to the improved tracking performance.

Fig. 3(a) shows the average positioning error versus horizontal antenna dimension. As can be seen, the average positioning error of co-sensing decreases with the N_y increase and is lower than that of separate sensing under different N_y. Fig. 3(b) shows that the proposed CSJT scheme is able to achieve higher average system sum-rate under different antennas. With the increase of N_y, the average system sum-rate of the CSJT scheme increases faster than the SSJT. Note that with a smaller ΔT, the tracking error is smaller; thus, the CSI can be updated more frequently and more accurately, which results in the increase of the gap between the sum-rate under $\Delta T = 0.02$s and that under $\Delta T = 0.05$s.

VI. Conclusion

In this paper, we studied co-sensing assisted JT for a multi-BS-to-multi-UAV communication system. In particular, we employed the EKF technique to predict the trajectories of UAVs, based on which, the BSs jointly transmit signals to UAVs. To improve the system sum-rate, we employed the TLBO algorithm to jointly design the transmit beam power of multiple BSs. Simulation results show that compared with the separate sensing scheme, the proposed co-sensing scheme is able to achieve more accurate tracking of UAVs, thereby enabling more efficient transmission strategy, and improving the system sum-rate.

References

[1] M. Mozaffari, W. Saad, M. Bennis, Y.-H. Nam, and M. Debbah, "A tutorial on UAVs for wireless networks: Applications, challenges, and open problems," *IEEE communications surveys & tutorials*, vol. 21, no. 3, pp. 2334–2360, 2019.

[2] Y. Li, N. I. Miridakis, T. A. Tsiftsis, G. Yang, and M. Xia, "Air-to-air communications beyond 5G: A novel 3D CoMP transmission scheme," *IEEE Transactions on Wireless Communications*, vol. 19, no. 11, pp. 7324–7338, 2020.

[3] H. Lee, S. Kim, and S. Lee, "Combinatorial orthogonal beamforming for joint processing and transmission," *IEEE Transactions on Communications*, vol. 62, no. 2, pp. 625–637, 2014.

[4] R. Amer, W. Saad, and N. Marchetti, "Mobility in the sky: Performance and mobility analysis for cellular-connected UAVs," *IEEE Transactions on Communications*, vol. 68, no. 5, pp. 3229–3246, 2020.

[5] F. Liu, W. Yuan, C. Masouros, and J. Yuan, "Radar-assisted predictive beamforming for vehicular links: Communication served by sensing," *IEEE Transactions on Wireless Communications*, vol. 19, no. 11, pp. 7704–7719, 2020.

[6] X. Wang, Z. Fei, J. A. Zhang, and J. Huang, "Sensing-assisted secure uplink communications with full-duplex base station," *IEEE Communications Letters*, vol. 26, no. 2, pp. 249–253, 2022.

[7] J. Mu, Y. Gong, F. Zhang, Y. Cui, F. Zheng, and X. Jing, "Integrated sensing and communication-enabled predictive beamforming with deep learning in vehicular networks," *IEEE Communications Letters*, vol. 25, no. 10, pp. 3301–3304, 2021.

[8] P. Liu, Z. Fei, X. Wang, J. A. Zhang, Z. Zheng, and Q. Zhang, "Securing multi-user uplink communications against mobile aerial eavesdropper via sensing," *IEEE Transactions on Vehicular Technology*, pp. 1–6, 2023.

[9] Q. Shi, L. Liu, S. Zhang, and S. Cui, "Device-free sensing in OFDM cellular network," *IEEE Journal on Selected Areas in Communications*, vol. 40, no. 6, pp. 1838–1853, 2022.

[10] Q. Zhang, H. Sun, X. Gao, X. Wang, and Z. Feng, "Time-division ISAC enabled connected automated vehicles cooperation algorithm design and performance evaluation," *IEEE Journal on Selected Areas in Communications*, vol. 40, no. 7, pp. 2206–2218, 2022.

[11] J. Wu, W. Yuan, F. Liu, Y. Cui, X. Meng, and H. Huang, "UAV-based target tracking: Integrating sensing into communication signals," in *2022 IEEE/CIC International Conference on Communications in China (ICCC Workshops)*. IEEE, 2022, pp. 309–313.

[12] A. A. A. El-Banna, M. Elsabrouty, A. Abdelrhman, and S. Sampei, "Low complexityadaptive detection of distributed sfbc in open-loop comp," in *2014 IEEE Symposium on Computers and Communications (ISCC)*. IEEE, 2014, pp. 1–5.

[13] K. Okubo, C.-J. Ahn, T. Omori, and K.-y. Hashimoto, "Enhancement of cell-edge throughput performance with comp transmission using qo-stbc scheme," in *2013 IEEE 2nd Global Conference on Consumer Electronics (GCCE)*. IEEE, 2013, pp. 496–499.

[14] M. S. Ali, E. Hossain, A. Al-Dweik, and D. I. Kim, "Downlink power allocation for CoMP-NOMA in multi-cell networks," *IEEE Transactions on Communications*, vol. 66, no. 9, pp. 3982–3998, 2018.

[15] J. Akhtar, "Doppler compensated space-time block coding for multi-static radar systems," in *2013 IEEE Radar Conference (RadarCon13)*. IEEE, 2013, pp. 1–5.

[16] B.-n. Vo, M. Mallick, Y. Bar-Shalom, S. Coraluppi, R. Osborne, R. Mahler, and B.-t. Vo, "Multitarget tracking," *Wiley encyclopedia of electrical and electronics engineering*, no. 2015, 2015.

[17] R. Rao and V. Patel, "An elitist teaching-learning-based optimization algorithm for solving complex constrained optimization problems," *international journal of industrial engineering computations*, vol. 3, no. 4, pp. 535–560, 2012.

[18] S. Mirbolouk, M. Valizadeh, M. C. Amirani, and S. Ali, "Relay selection and power allocation for energy efficiency maximization in hybrid satellite-UAV networks with CoMP-NOMA transmission," *IEEE Transactions on Vehicular Technology*, vol. 71, no. 5, pp. 5087–5100, 2022.